



<http://www.diva-portal.org>

Postprint

This is the accepted version of a paper presented at *PVSEC-23; 23rd International Photovoltaic Science and Engineering Conference; Taipei, Taiwan; October 28 - Nov 1, 2013.*

Citation for the original published paper:

Frisk, C., Platzer-Björkman, C., Fjällström, V., Salomé, P., Olsson, J. et al. (2013)

Modeling Ga-profiles for Cu(In,Ga)Se₂ thin film solar cells with varying defect density.

In: *23rd International Photovoltaic Science and Engineering Conference; Taipei, Taiwan; October 28 - Nov 1, 2013: Proceedings*

N.B. When citing this work, cite the original published paper.

Permanent link to this version:

<http://urn.kb.se/resolve?urn=urn:nbn:se:uu:diva-211669>

Modeling Ga-profiles for Cu(In,Ga)Se₂ thin film solar cells with varying defect density

C. Frisk*, C. Platzer-Björkman, V. Fjällström, P. Salomé, J. Olsson, M. Edoff

Ångström Solar Center, Division of Solid State Electronics, Uppsala University
Box 534, SE-751 21, Uppsala, Sweden

*christopher.frisk@angstrom.uu.se

ABSTRACT

The very best Cu(In,Ga)(S,Se)₂ solar cells have a double graded band gap in the absorber, i.e. a notch profile, formed by varying the ratio of Ga to In. If this is a prerequisite or a consequence of high quality deposition methods is something yet of discussion. In this work we have constructed a high efficiency model (HE-T61) based on in-house state-of-the art Cu(In,Ga)Se₂ solar cells, with efficiencies above 19 %, and investigated the role of the Ga-profile. Notch-type Ga-profiles have been compared with single graded profiles, and the influence of Ga-dependent defect distribution and metastable defects have been investigated showing that the optimum Ga-profile is dependent on such defect variations. It is also shown that within the HE-T61 model the optimized Ga-profile yields up to 3 % absolute efficiency gain, indicating that there is potential in band gap engineering. *Errata: See footnote.*

1. INTRODUCTION

Today many of the high efficiency Cu(In,Ga)(S,Se)₂ (CIGS) thin film solar cells are engineered to have band gap gradients in the absorber layer. This can be done by altering the group three element ratio, $GGI = \frac{Ga}{Ga+In}$, where higher GGI mainly increases the conduction band edge energy^[1]. Thus, increasing GGI towards the back interface improves the current collection and reduces the back surface recombination, and increasing GGI towards the front interface reduces recombination in the space charge region (SCR) and can increase the open circuit voltage (V_{oc}). We refer to GGI throughout the absorber as a Ga-profile.

Top efficiency CIGS solar cells have notch structured Ga-profiles^[2,3], i.e. with both a back and front grading. In the three-stage process, known for being a high quality deposition method, the notch is formed by consequence. But is it a prerequisite for high efficiency CIGS in general?

In this work we have investigated the role of the Ga-profile in a new SCAPS^[4] model, with

input data from one representative state-of-the art in-house CIGS solar cell. The cell was made with an in-line simulated co-evaporation process (T61), engineered to produce a high current while maintaining a relatively high voltage ($\eta > 19\%$). The layers of T61 were nominally 2 mm SL glass, 750 nm Mo, 15 nm NaF, 2.16 μ m Cu(In,Ga)Se₂, 50 nm CdS, 80 nm i:ZnO, 165 nm Al:ZnO, and Ni/Al/Ni grid with 140 nm MgF₂ antireflective (AR) coating on the top.

Starting with our high efficiency T61 (HE-T61) model, which was designed to correspond to the representative T61 solar cell in a simple but realistic way, we aimed for three goals (recurring in section 2 and 3):

- i) To find an optimum notch Ga-profile (O-N), and comparing it to an optimum single graded profile (O-SG) within the HE-T61 model.
- ii) To compare respective strengths and limitations of notch and single graded profiles.
- iii) To extend the HE-T61 model and see how other types of defect variations affects the choice of optimized Ga-profiles (marked with *). These variations include metastable defects and Ga-dependent defect density.

Errata: In these simulations the radiative recombination coefficient was set to zero. This error does not influence the results of the simulations with the exception of the most extreme Ga-profile (O-N). The radiative recombination will be considered in future simulations. Thanks to Hiroki Sugimoto from Solar Frontier by whom this error was noted during the conference.

2. EXPERIMENTAL

2.1 High Efficiency T61 model

In our HE-T61 SCAPS model most of the parameters were taken from our in-house baseline model^[5], based on similarly produced cells. The parameters that were changed are discussed below.

The thickness of the CIGS was measured with PANalytical Epsilon 5 X-ray fluorescence analyzer (XRF), calibrated with a Nanotech Dektak Stylus Profilometer. By comparing the simulated EQE with measured EQE the CdS buffer layer thickness was concluded to be around 75 nm. The values can be seen in Table 1.

The stack reflectance was measured with a Perkin Elmer 900 photo spectrometer with integrating sphere. The measurement was done on the full stack with grid and scribe lines.

The Ga-profile was measured with glow discharge optical emission spectroscopy (GD-OES) using a SPECTRUMA GDA-750 Analyzer, calibrated with XRF. However, by comparing GGI from XRF data of flat profiles with calculated GGI from the absorption edge of respective EQE measurement, it was found that the GGI was consistently 5 % lower. Thus, the HE-T61 GD-OES profile was also lowered 5 %.

The CIGS doping was estimated from drive-level capacitance profiling (DLCP) at room temperature. In light soaked state, $N_{A,ls} = 7 \cdot 10^{15} \text{ cm}^{-3}$ and in relaxed state, $N_{A,r} = 3 \cdot 10^{15} \text{ cm}^{-3}$ (used in extended model).

The bulk defects in the CIGS were assumed to be p-type at mid-gap, chosen as equivalent recombination centers with a density of $N_T = 3 \cdot 10^{12} \text{ cm}^{-3}$. The value comes from comparing simulated and measured JV parameters.

The interface defects between absorber and buffer were assumed to be n-type at mid-gap with a density $N_{IT} = 3 \cdot 10^{11} \text{ cm}^{-2}$, chosen in the same fashion as the bulk defects.

Shunt conductance, $\sigma_{sh} = 1 \text{ mS cm}^{-2}$, and *series resistance*, $R_s = 0.3 \text{ } \Omega \text{ cm}^2$, were extracted from the measured JV-data using the method of Hegedus and Sharfarman^[6].

Table 1: The thickness, doping and defect density of each layer of the HE-T61 SCAPS model. (p/n) denotes p/n-type doping.

Layer	Thickness	Doping [cm^{-3}]	Defects [cm^{-3}]
CIGS	2.16 μm	$7 \cdot 10^{15}$ (p)	$3 \cdot 10^{12}$ (0/-)
CdS	75 nm	$5 \cdot 10^{17}$ (n)	$2 \cdot 10^{17}$ (+/0)
i:ZnO	80 nm	10^{17} (n)	10^{16} (+/0)
Al:ZnO	165 nm	10^{20} (n)	10^{16} (+/0)

Table 2: The JV parameters of the T61 cell, the HE-T61 model and subsequent optimized models.

Name	V_{oc} [mV]	J_{sc} [mA cm^{-2}]	FF [%]	η [%]
T61	685	36.8	75.9	19.1
HE-T61	673	37.8	76.8	19.5
O-SG	787	34.3	77.7	21.0
O-N	877	36.0	71.1	22.5
O-SG*	749	34.8	78.3	20.4
O-N*	782	34.0	76.7	20.4

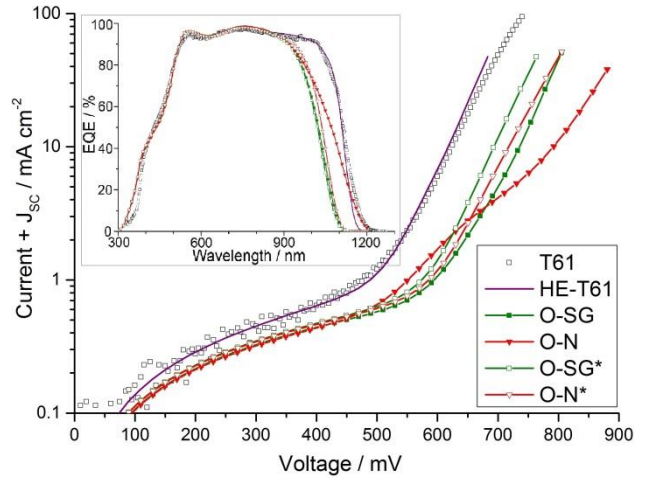


Figure 1: The JV simulation and measurement data. The O-N profile is distinguished by the low fill factor due to the barrier formed by the notch. The inset shows the QE of respective samples.

The HE-T61 model was considered to fit well with measurements with only small differences in V_{oc} , short circuit current (J_{sc}) and fill factor (FF), see Table 2, and respective JV and EQE graph can be seen in Figure 1. It should be noted that V_{oc} is limited by the absorber doping and the Ga-profile in HE-T61, since V_{oc} cannot be substantially increased even by setting the defect densities to zero. The higher J_{sc} in the model might be due to non-ideal or dead areas.

2.2 Simulations

i) The optimum single graded Ga-profile, O-SG, was found by varying GGI at front and back interface. The optimum notch Ga-profile, O-N, was found by additionally varying the

Errata: In these simulations the radiative recombination coefficient was set to zero. This error does not influence the results of the simulations with the exception of the most extreme Ga-profile (O-N). The radiative recombination will be considered in future simulations. Thanks to Hiroki Sugimoto from Solar Frontier by whom this error was noted during the conference.

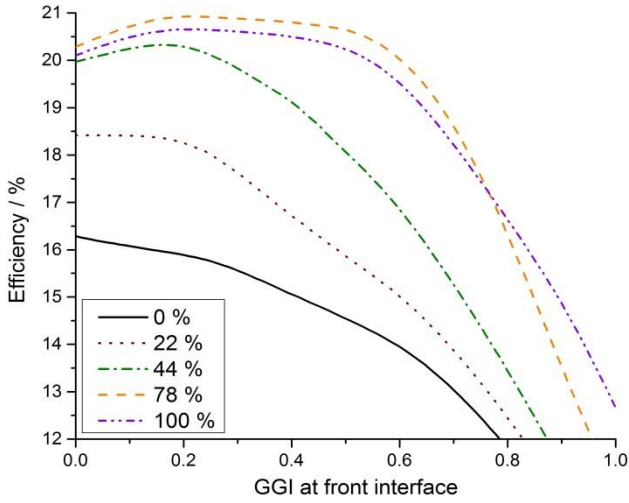


Figure 2: Single graded Ga-profile optimization process, where the GGI at the front (x-axis) and back (legend) interface has been varied.

position of the notch from respective interface and GGI at the notch. An example of the optimization simulation can be seen in Figure 2.

ii) The comparison between non-optimized single graded and notch profiles was done by looking at simulated JV-parameters, and modeling the recombination at forward bias, while varying bulk and interface defect densities 10^{12} – 10^{15} cm^{-3} and 10^{10} – 10^{12} cm^{-2} respectively.

iii) The model was extended by implementing a Ga-dependent defect distribution according to previous findings^[7], with minimum of $3 \cdot 10^{12}$ cm^{-3} at GGI = 0.3, since it is commonly known that the quality of CIGS drops with GGI above 30%^[8], and a maximum of 10^{14} cm^{-3} at GGI = 1. Moreover, temperature dependent DLCP measurement of T61 exhibited higher doping after light soaking. Such light-induced metastable behavior has been suggested to originate from the Se-Cu di-vacancy complex^[9]. Thus, this defect as treated in previous modeling^[4] was added to the extended model, with electron/hole capture and emission energies from an experimental investigation^[10]. In this case, the measured relaxed doping density $N_{A,r}$ was used. The optimum Ga-profiles were expected to change with above extensions, and the new optimum notch (O-N*) and single graded (O-SG*) profile was investigated.

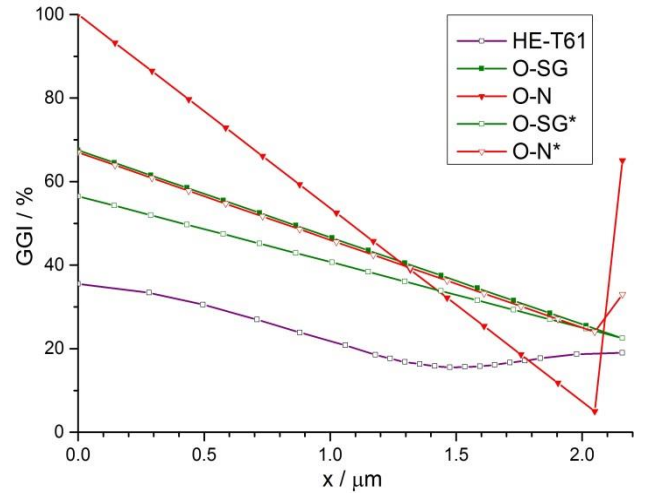


Figure 3: The Ga-profiles of the absorber, measured with GD-OES for the T61 cell (and the HE-T61 model), and modeled in the other cases.

3. RESULTS AND DISCUSSIONS

i) It is possible to optimize the Ga-profile in the HE-T61 model, see O-N in Figure 3, gaining about 3 % efficiency, see Table 2. The increase is attributed both to a more pronounced grading and an overall increase in band gap. As expected the increase lies in V_{oc} , and the slight loss of J_{sc} is downplayed. Comparing O-N with O-SG, both V_{oc} and J_{sc} are higher for O-N, and even if the FF is higher for O-SG, the overall efficiency is more than 1 % higher for the notch profile. To note is the challenge to deposit such a sharp profile and shallow notch, due to temperature and reaction driven diffusion during growth.

ii) Simulations show that recombination can increase at the notch, e.g. caused by accumulation of free electrons and a low band gap. This weakness is not prominent when the notch is placed in the SCR, compared to when the notch is placed deeper in the absorber, acknowledged in other works as well^[11].

For single graded profiles most of the recombination occurs in the SCR and at the interface, true also with notches placed in the SCR. However, changing the interface defect density has larger impact on single graded profiles; lowering interface defect density drastically increases the efficiency (V_{oc}) at low bulk defect density, whereas the increase of efficiency for the notch profile in the same case is negligible. Increasing the bulk defect density

instead reduces the notch profile efficiency more than for the single graded profile, to a point where a single graded profile is more efficient. However, none of these profiles were specifically optimized to each and every defect variation. This shows that the optimum profile type is strongly dependent on absorber defect distribution. There is no unique best Ga-profile, and not even a unique best profile type.

iii) Extending the model with a Ga-dependent defect distribution lowered the efficiency around 0.25 % for O-SG and 1 % for O-N, mainly due to a drop in V_{oc} caused by an overall increase of defects, especially close to the interface in the case of O-N. The efficiency could in neither case be increased by altering the Ga-profiles. Implementing the metastable defect complex has a larger impact, where the deep acceptor state at 0.85 eV traps electrons at forward bias and reduces V_{oc} . O-SG dropped an additional 0.8 % in efficiency, while O-N decreased another 2.3 %. The Ga-profiles could in this case be re-optimized (O-N* and O-SG*, found in Figure 3); a higher GGI at the notch proved favorable, increasing efficiency by 1.2 % owing to an improvement of V_{oc} and FF, while insignificant efficiency gains were obtained by lowering GGI at the back interface (both profiles) and at the front interface (O-N*). This effect was not altered by changing the transition energy of the metastable defects. In the extended model the efficiency of O-SG* was comparable to that of O-N*, see Table 2.

4. CONCLUSIONS

In this work a SCAPS model (HE-T61) has been created based on highly efficient CIGS solar cells (T61), with consistency between simulations and experimental data. The influence of Ga-profiles has been investigated and the optimum single graded and notch profiles have been found within HE-T61, improving efficiency around 3 % with the best notch profile. This indicates that there is room for improvement in our T61 process, mainly by

increasing the overall Ga-ratio, even if there are some difficulties to deposit such profiles. The HE-T61 model was also extended with Ga-dependent defect density and metastable defects. Within the extended model the efficiency gain by optimizing the Ga-profile was limited to 1 %, mainly due to deep acceptor trap levels. This study shows that notch-type Ga-profiles not always yield highest efficiency, and that the choice of Ga-profile is strongly dependent on defect type and distribution.

ACKNOWLEDGEMENT

The author gratefully acknowledges the support from Mark Burgelman, who supplied a reference SCAPS definition file, the Solid State Physics department for optical measurements, and the Swedish Research Council for funding.

REFERENCES

- [1] S.-H. Wei, S. B. Zhang and A. Zunger, *Appl. Phys. Lett.*, **72** (1998), 3199
- [2] Adrian Chirilă *et al.*, *Nature Materials* **10** (2011), 857
- [3] P. Jackson, D. Hariskos, E. Lotter, S. Paetel, R. Wuerz, R. Menner, W. Wischmann and M. Powalla, *Prog. Photovolt: Res. Appl.* **19** (2011), 894
- [4] M. Burgelman, K. Decock, S. Khelifi and A. Abass, *Thin Solid Films*, **535** (2013), 296
- [5] J. Pettersson, C. Plazer-Björkman, U. Zimmermann and M. Edoff, *Thin Solid Films* **519** (2011), 7476
- [6] S.S Hedgedus and W. N. Shafarman, *Prog. Photovolt: Res. Appl.* **12** (2004), 155
- [7] G. Hanna, A. Jasenek, U. Rau and H.W. Schock, *Thin Solid Films* **387** (2001), 71
- [8] W. N. Shafarman and L. Stolt, *Handbook of Photovoltaic Science and Engineering*, Ch. 13, p. 567, John Wiley Sons Ltd., 2003
- [9] S. Lany and A. Zunger, *J. Appl. Phys.*, **100** (2006), 113725
- [10] A. Urbaniak and M. Igalson, *J. Appl. Phys.*, **106** (2009), 063720
- [11] M. Pawlowski, P. Zabierowski, R. Bacewicz and N. Barreau, *Thin Solid Films*, **535** (2013), 226